Principal Component Analysis of Two-dimensional Flow Vector Fields on Human Facial Skin for Efficient Robot Face Design

Nobuyuki Ota, Hisashi Ishihara, and Minoru Asada

Graduate School of Engineering, Osaka University

Abstract. In this study, deformation patterns of an adult male lower face are measured and analyzed for efficient face design for android robots. We measured flow vectors for 96 points on the right half of the lower face for 16 deformation patterns, which are selected from Ekman's action units. Namely, we measured 16 flow vector fields of facial skin flow. The flow vectors were created by placing ink markers on the front of the face and then video filming various facial motions. A superimposed image of vector fields shows that each point moves in various directions. Principle component analysis was conducted on the superimposed vectors and the contribution ratio of the first principal component was found to be 86%. This result suggests that each facial point moves almost only in one direction and different deformation patterns are created by different combinations of moving lengths. Based on this observation, replicating various kinds of facial expressions on a robot face might be easy because an actuation mechanism that moves a single facial surface point in one direction can be simple and compact.

1 Introduction

Facial expression is one of the important communication channels for humans; therefore, designers of communication robots have tried to replicate human facial expressions on robot faces [1, 2, 4–14]. When humans change facial expressions, entire skin surfaces deform in complicated patterns, which is difficult for robot designers to replicate. To replicate several facial expressions on a single robot face, the designers should know how each point on a human face moves for several facial deformation patterns.

Traditionally, robot face designers [2, 4, 6, 7, 10, 11, 13, 14] have decided the locations of facial moving points and their directions based on Ekman's action units (AUs), which are summarized and introduced in the Facial Action Coding System (FACS) [3]. AUs are facial deformation patterns created when one or more facial muscles are activated, and FACS explains that different facial expressions are realized by different combinations of one or several action units.

However, AUs are not enough to design effective actuation mechanisms for a robot face because only verbal qualitative descriptions of deformations are introduced in FACS. Instead, quantitative information such as flow vector fields must be used to effectively design robot faces. Cheng et al.[2] have pointed out this issue and measured facial deformations with a 3D scanner. However, their observation was limited to only four typical facial expressions, which were smile, anger, sadness, and shock.

Therefore, in this study, we measured every conceivable deformation pattern especially in the lower face of a Japanese adult male. Namely, we measured flow vector fields of facial skin. Then, two kinds of compensation processing for the measured vector fields, such as head movement compensation and neutral face matching, are executed. Finally, Principal Component Analysis (PCA) was conducted to determine variations in movements and flow field trends of each facial point.

2 Method

2.1 Motion Patterns

FACS introduces sixteen deformation patterns in the lower face and they are selected for this experiment. Table 1 summarizes the selected deformation patterns. Each AU has its own AU number and name defined in FACS. Basically, the name contains information about the responsible part of the face (e.g., lip corner) and its deformation pattern (e.g., puller).

FACS describes how to activate each AU and an example of its associated facial image. A Japanese adult male (hereafter demonstrator) activated each AU and his facial deformations were measured in this experiment.

Table 1. deformation patterns (Ekman's action units) measured in this experiment

AU Number	Name
9	Nose Wrinkler
10	Upper Lip Raiser
11	Nasolabial Furrow Deepener
12	Lip Corner Puller
13	Sharp Lip Puller
14	Dimpler
15	Lip Corner Depressor
16	Lower Lip Depressor
17	Chin Raiser
18	Lip Pucker
20	Lip Stretcher
22	Lip Funneler
23	Lip Tightener
24	Lip Presser
25	Lips Part
28	Lips Suck

2.2 Measurement

Ninety six measurement points were identified on the demonstrator's skin, and ink markers were placed on them, as shown in Fig.1. Each marker was approximately 2-5 mm in size, and their locations were decided so that they were placed not only on anatomically distinctive points, such as corners of the mouth and the top of the nose, but also on other plane surfaces such as the cheek.

The movements (or flows) of the markers for each AU were recorded by video filming (SONY HANDYCAM HDR-CX420) at the front of the demonstrator. While being filmed, the demonstrator began with a neutral face, activated one of the selected AUs, and kept its deformation for several seconds. Sixteen video recordings were created, each of which contains both the demonstrator's neutral face and his deformed one.

Fig. 1. Locations of ink markers on the right half of a Japanese adult male's lower face

2.3 Data Processing

To measure flow vectors of the markers, two video frames were selected from each video recording of each AU. The first one contains the demonstrator's neutral face and the second one contains his deformed one.

By comparing pixel coordinates of each marker in these two images, we can roughly calculate each marker's flow vector. However, two kinds of image corrections are necessary to calculate more precise flow vectors and to superimpose several flow vectors of the same marker. The first one is the Head Movement Compensation. While activating each AU, the demonstrator's head can move; therefore, the markers' pixel coordinates can move even if the marker does not move on face. The second one is Neutral Face Matching between different AUs to superimpose several vectors for the same marker. Even though the demonstrator tried to show the same neutral face with the same head position in each video recording session, these neutral faces can not be exactly the same. Therefore, starting points for flow vectors of the same marker are not in the same position between different AUs.

Head Movement Compensation For head movement compensation, five reference points on the facial images shown in Fig. 2 were used. Reference points were placed on the top of the nose, on the mid-point between the eyes, and on the mid-point between the corner of the eye and the ear. These points are known to be relatively static on humans faces[2]. In addition to these three points, two additional reference points were placed on the top of the head and the chin.

The sizes and positions of the two images for each AU were adjusted so that each reference point matched. This adjustment was manual because matching five points was relatively simple.

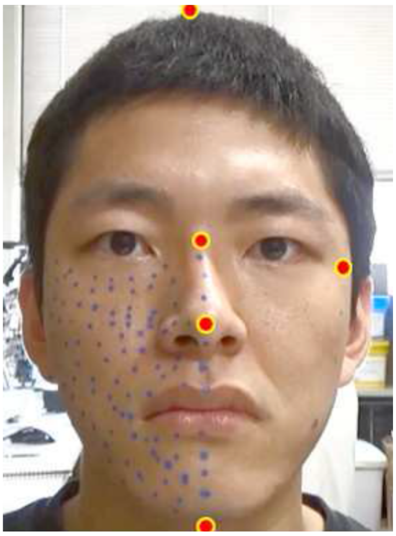

Fig. 2. Reference points on a facial image for head movement compensation

Neutral Face Matching For neutral face matching between different AUs, first, the neutral face image for AU9 was randomly chosen as a reference image. Affine transformations were applied to 15 sets of 97 marker coordinates (96 ink markers and the reference point on the top of the chin) in neutral face images so that these marker sets would match with a marker set of the reference image.

Two-dimensional coordinate vector $X_{i,j}$ of a marker i in an image j is converted to a coordinate vector $X'_{i,j}$ by the equation

$$X'_{i,j} = A_j X_{i,j} + b_j,$$

where A_j is a linear transformation matrix and b_j is a translation vector for an image j. The purpose is to find the parameters of A_j and b_j so that the coordinate vectors $X'_{i,j}(i = 1, \ldots, 97)$ match with vectors $X_{i,9}$ for an neutral face image of AU9.

To find the appropriate parameters, Steepest Descent Method was implemented with an error function defined as

$$F(A_j) = \sqrt{\Sigma_{i=1}^{97} \|X_{i,9} - X'_{i,j}\|^2} \ .$$

3 Result

3.1 Flow Vector Fields

Figures 3 and 4 show the measured flow vector fields for AU12 and AU16, respectively. Green arrows represent flow vectors, and the facial images depict deformation for each AU. These flow vectors were obtained after the Head Movement Compensation. After the compensation, the maximum average error of five reference points between two images was 1.9 pixels. Considering the actual head size was 275 mm and the head image size was 600 pixels, the estimated error was 0.9 mm.

These figures show how facial deformations are extensive and complicated and how the flow fields are different between AUs. For example, in AU12, which is Lip Corner Puller, we can see entire surfaces around the cheek, lips, and jaw move. The flow vectors near the lip corner have longer lengths, and their directions are aligned toward the top side of the face. On the other hand, in AU16, which is Lower Lip Depressor, we can see the entire surface below the mouth movement, and these directions are not aligned toward the side bottom.

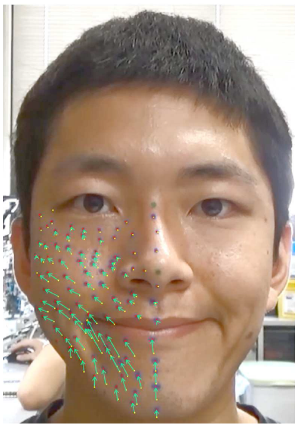

Fig. 3. Measured skin flow vector field for AU12 (Lip Corner Puller)

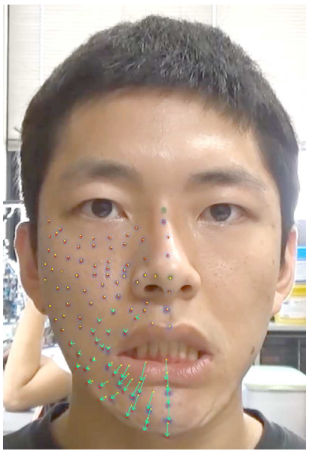

Fig. 4. Measured skin flow vector field for AU16 (Lower Lip Depressor)

3.2 Superimposed Field

Figure 5 represents the superimposed vector field before Natural Face Matching, which is the compensation processing to match vector starting points for the same marker. Vector colors indicate the vector angle. We can find that the starting points are not matched.

On the other hand, the starting points are matched well after Neutral Face Matching, as shown in Figure 6. From this figure, we can determine how far and in which directions each point on the face moved. The point near the face midline moved only vertically. However, other points moved in several directions. The points near the mouth moved farther than points near the nose or the eye. The maximum vector length was 22 mm and it appeared at the corner of the lower lip for AU13.

Thus, the flow vectors seem to be too complex to replicate on a robot face. However, there seems to be a trend in the flow lines that connect the chin, the corner of the eye, and the corner of the lips. We will analyze this trend in the next section.

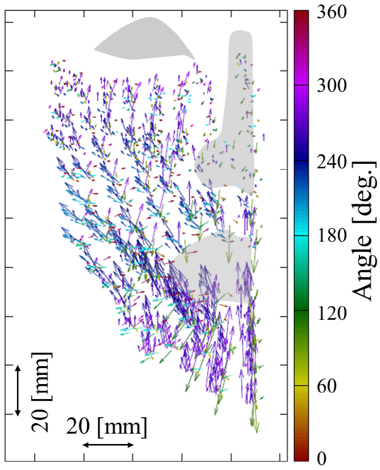

Fig. 5. Superimposed vector field before Neutral Face Matching. Starting points are not matched. The positions of the eye, nose, and mouth are indicated by gray areas as a reference.

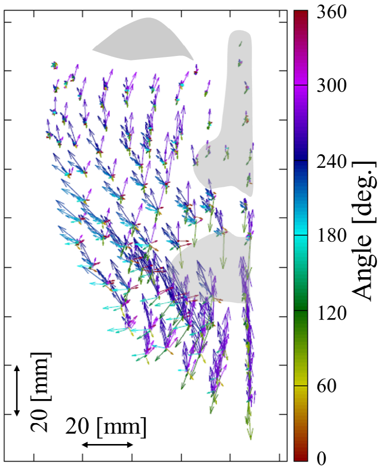

Fig. 6. Superimposed vector field after Neutral Face Matching. Starting points are matched. The positions of the eye, nose, and mouth are indicated by gray areas as a reference.

3.3 Principal Component Analysis

Figure 7 shows the first and second principal components of each marker's flow vectors whose starting points are matched by Neutral Face Matching. The directions of two double-headed arrows for each marker represent the directions of the first and second principal components, respectively, while the lengths of the two arrows represent the variances of their scores. Namely, the longer the arrows, the farther the marker moved for different AUs. We found that the arrows closer to the mouth are longer.

Figure 8 shows the histogram for the contribution ratios of the first principal components for every marker. Their average was 86%, which means that almost all marker movement occur only in one direction at each point.

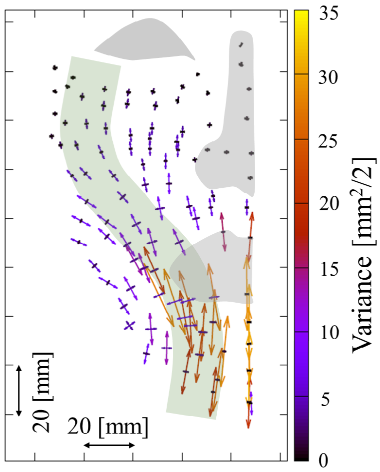

Fig. 7. The first and second principal components of flow vectors for each marker. The directions of two double-headed arrows for each marker represent the directions of the first and second principal components, respectively, while the lengths of the two arrows represent variances of their scores. The positions of the eye, nose, and mouth are indicated by gray areas as a reference. The s-shape trend of the flow lines is indicated by a green line.

Figure 9 shows the histogram for the minimum reproduction errors of every flow vectors when every markers move only in the directions of each first principal component. The reproduction error of each marker in each AU is its second principal component score. Over eighty percent of the reproduction errors was under 2 [mm] and over 95 percent of them was under 4 [mm].

Furthermore, we can find an s-shape trend of flow lines that connect the side of the chin, the corner of the lips, the side of the cheek, and the corner of the eye. This trend is represented in Fig. 7 as a green line.

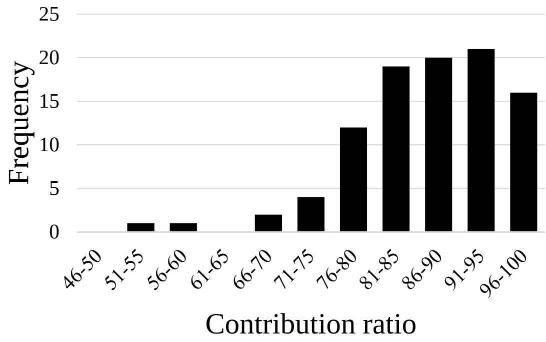

Fig. 8. Histogram for the contribution ratios of the first principal components for every marker

4 Conclusion

The main findings of the measurement and analysis of 16 patterns of facial flow vector fields are as follows:

- Although facial surfaces seem to move in a complicated manner when several deformation patterns are expressed, almost all movements occur only in one direction in each measured point on the face.
- Such principal directions for all of the points are continuous through the entire facial surface; such continuous flows form an s-shape trend.
- Moving lengths for each point for several deformation patterns vary more significantly around the mouth.

These findings suggest that various kinds of facial expressions are created by combinations of different movement lengths of facial surface points, each of which moves almost only in one direction.

These observations can facilitate replicating various kinds of facial expressions on a robot. This is because an actuation mechanism that moves a facial surface point in one direction can be simple and compact while a mechanism that moves the point in several directions would be complex.

However, several problems remain to be solved to obtain further effective design policies for face robots. First, the flow vectors lack depth information since we obtained these vectors from two-dimensional images. Therefore, three-dimensional flow vectors should be obtained for more precise analysis. Second, the number of points required to replicate the flow vector fields on a robot should be less than 96 because that is too many to prepare actuation mechanisms for each point. Therefore, neighbor points that move similarly should be treated as a single point representing its peripheral area. Third, the second principal component should not be ignored. Although its contribution ratio is low, skin

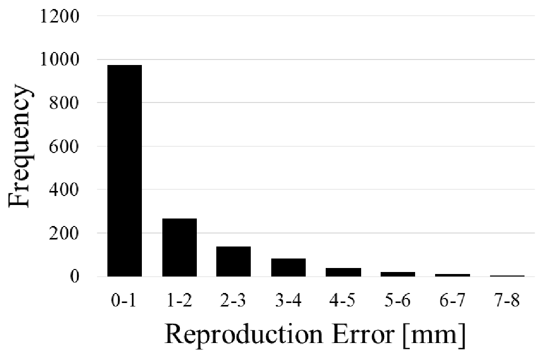

Fig. 9. Histogram for the reproduction errors of flow vectors when every markers move only in the directions of each first principal component

flows of the second principal component exist and they can be dominant in some of deformation patterns. Further flow field analyses are necessary on each AU to understand when flows of the second principal component occur.

Acknowledgment

This work was supported by a Grant-in-Aid for Specially Promoted Research No. 24000012 and for Young Scientist (B) No. 15K18006.

References

1. Bickel, B., Kaufmann, P., M., S., Thomaszewski, B., Bradley, D., Beeler, T., Jackson, P., Marschner, S., Matusik, W., Gross, M.: Physical Face Cloning. ACM Transactions on Graphics 31(4), 118:1–118:10 (2012)
2. Cheng, L.C., Lin, C.Y., Huang, C.C.: Visualization of Facial Expression Deformation Applied to the Mechanism Improvement of Face Robot. International Journal of Social Robotics 5(4), 423–439 (2013)
3. Ekman, P., Friesen, W.V., Hager, J.C.: Facial Action Coding System (FACS): Manual. In: A Human Face (2002)
4. Hanson, D., Andrew, O., Pereira, I.A., Zielke, M.: Upending the uncanny valley. In: Proc. International Conference on Artificial Intelligence (2005)
5. Hashimoto, M., Yokogawa, C.: Development and Control of a Face Robot Imitating Human Muscular Structures. In: Proc. International Conference on Intelligent Robots and Systems. pp. 1855–1860 (2006)
6. Hashimoto, T., Hiramatsu, S., Kobayashi, H.: Development of Face Robot for Emotional Communication between Human and Robot. In: Proc. International Conference on Mechatronics and Automaton. pp. 25–30 (2006)
7. Hirth, J., Schmitz, N., Berns, K.: Emotional architecture for the humanoid robot head ROMAN. In: Proc. International Conference on Robotics and Automation. pp. 2150–2155 (2007)
8. Ishiguro, H.: Android science: conscious and subconscious recognition. Connection Science 18(4), 319–332 (2006)
9. Ishihara, H., Yoshikawa, Y., Asada, M.: Realistic child robot "Affetto" for understanding the caregiver-child attachment relationship that guides the child development. In: IEEE Proc. International Conference on Development and Learning. pp. 1–5 (2011)
10. Kobayashi, K., Akasawa, H., Hara, F.: Study on new face robot platform for robot-human communication. In: 8th International Workshop on Robot and Human Interaction. pp. 242–247 (1999)
11. Lin, C.Y., Cheng, L.C., Tseng, C.K., Gu, H.Y., Chung, K.L., Fahn, C.S., Lu, K.J., Chang, C.C.: A face robot for autonomous simplified musical notation reading and singing. Robotics and Autonomous Systems 59(11), 943–953 (2011)
12. Minato, T., Yoshikawa, Y., Noda, T., Ikemoto, S., Ishiguro, H., Asada, M.: CB2: A child robot with biomimetic body for cognitive developmental robotics. Proc. the 7th IEEE-RAS International Conference on Humanoid Robots pp. 557–562 (2007)
13. Tadesse, Y., Priya, S.: Graphical Facial Expression Analysis and Design Method: An Approach to Determine Humanoid Skin Deformation. Journal of Mechanisms and Robotics 4(2), 1–16 (2012)
14. Yu, Z., Ma, G., Huang, Q.: Modeling and design of a humanoid robotic face based on an active drive points model. Advanced Robotics 28(6), 379–388 (2014)